

Actinide Neutron-Induced Fission up to 200 MeV

Vladimir MASLOV^{1*}, Yuriy PORODZINSKI¹, Mamoru BABA²,
Akira HASEGAWA³

¹Radiation Physics and Chemistry Problems Institute, 220109, Minsk-Sosny, Belarus

²Cyclotron and Radioisotope Center, Tohoku University, Aoba-ku, Sendai 980-8578, Japan

³Japan Atomic Energy Research Institute, Tokai-mura, Ibaraki 319-1106, Japan

Neutron-induced fission cross sections of U, Np and Pu target nuclides are analyzed in fission/evaporation approximation up to 200 MeV excitation energy. Damping of collective modes contribution to the level density at excitation energies higher than ~ 20 MeV for saddle and equilibrium deformations is shown to be essential. Effective estimates of intrinsic level densities are obtained. Actinide first-chance fission cross sections of $^{238}\text{U}(n,f)$ and $^{238}\text{U}(p,f)$ reactions are found to be much different. Differences of measured proton- and neutron-induced fission cross sections of ^{238}U are attributed to the influence of the isovector term of the nucleon-nucleus optical potential.

KEYWORDS: nucleon-induced fission, actinides, intermediate energies

I. Introduction

High energy neutron-induced fission cross section measured data for ^{232}Th , ^{238}U , ^{235}U , ^{233}U , ^{237}Np , ^{239}Pu , ^{240}Pu , ^{242}Pu , ^{244}Pu ¹⁻³⁾ provide a possibility to check the adequacy of statistical theory of nuclear reactions for up to $E_n \sim 200$ MeV. However, the situation is complicated by the data discrepancies even below $E_n \sim 20$ MeV, which questions the data reliability at higher E_n . Main controversial point is dependence of fission cross section at $E_n \sim 100$ -200 MeV on the target fissility. It is evident for the ^{232}Th , but it is much less certain for the higher fissility targets. Another controversial point is the reason of difference of p - and n -induced fission cross sections at $E_{n(p)} \sim 40$ -200 MeV,^{4,5)} the latter being appreciably lower. Since it was claimed⁵⁾ that total inelastic cross section for protons is lower than that for neutrons, it was difficult then to interpret the ratio of $\sigma(n,f)/\sigma(p,f) < 1$ above $E_{n(p)} \sim 40$ MeV. The difference of measured data is much pronounced in case of $^{238}\text{U}(p,f)$ and $^{238}\text{U}(n,f)$ reactions.

Calculated fission cross section is a complex function of compound nucleus formation cross section, fission barrier parameters, intrinsic and collective modes contributions to the level density at equilibrium and saddle-point deformations for nuclei emerging in the decay chain. With the collective enhancement effects included into level density calculations actinide neutron-induced fission cross section data could be reproduced up to ~ 20 MeV.^{6,7)} At higher excitation energies we would probe the damping of the collective enhancement both at saddle and equilibrium deformations and check the σ_{nf} cross section sensitivity to the intrinsic level densities and fission barriers.

II. The Model

The statistical model of fission cross section assumes fission/evaporation competition during the decay of excited compound nucleus, which is formed after emission of first pre-equilibrium neutron. We use a modified version of

Hauser-Feshbach statistical model code STAPRE.⁸⁾ Fission decay widths were calculated within double-humped fission barrier model. Level density, main ingredient of fission and neutron decay calculation, is described elsewhere.^{6,7,9)}

1. Nucleon Optical Potential

A coupled channel model is adopted here for the calculation of neutron reaction cross section. To obtain a reasonable estimate of reaction cross section, we assumed that it should be kept at least above the highest fission cross section. We obtained optical potential parameters with $0^+ - 2^+ - 4^+ - 6^+ - 8^+$ coupling scheme within rigid rotator model fitting total data¹⁰⁾ up to $E_n \sim 200$ MeV. The neutron optical potential parameters are as follows (E_n, V, W - in (MeV), r, a - in (fm):

$$V_R^n = 45.93 - 0.28E_n + 0.000573E_n^2,$$

$$r_R = 1.26, a_R = 0.63, r_D = 1.26, a_D = 0.52$$

$$W_D^n = \begin{cases} 3.14 + 0.436E_n, & E_n \leq 8 \text{ MeV}, \\ 6.628 \text{ MeV}, & 8 < E_n < 20 \text{ MeV} \\ 8.368 - 0.091E_n + 0.0002E_n^2, & E_n \geq 20 \text{ MeV}, \end{cases}$$

$$W_C^n = \begin{cases} 0, & E_n \leq 30 \text{ MeV}, \\ 0.07(E_n - 30) \text{ MeV}, & E_n < 125 \text{ MeV} \\ 6.65 + 0.03325(E_n - 125), & \text{MeV}, E_n > 125 \text{ MeV} \end{cases}$$

$$r_C = 1.246 \text{ fm}, a_C = 0.2 \text{ fm}$$

$$V_{SO} = 6.2 \text{ MeV}, r_{SO} = 1.12, a_{SO} = 0.47,$$

$$\beta_2 = 0.195, \beta_4 = 0.078$$

Above $E_n \sim 10$ MeV shapes of total and reaction cross sections are different from those, calculated with potential by Young.¹¹⁾ Adopting rather weak volume absorption term W_C^n we obtained consistent description of fission and (n, xn) reaction data above $E_n \sim 10$ MeV.¹²⁾

It is generally supposed that to predict proton-nucleus reaction cross section using neutron-nucleus optical potential one needs to determine the isovector term of the latter¹³⁾ as well as Coulomb correction for protons. Actually, both real V_R^n and imaginary surface W_D^n terms have isovector terms, which depend on the symmetry parameter $\gamma = (N - Z)/A$. Values of $V_R^{n(p)}$ and $W_D^{n(p)}$ are calculated for neutrons and protons with opposite signs of these isovector terms, that is

* Corresponding author, Tel./Fax. +375-2467341, E-mail: maslov@sosny.bas-net.by, maslov@bas-net.by

$V_R^p = V_R^n - 2\alpha\gamma$, $W_D^p = W_D^n - 2\beta\gamma$, where α and β are parameters, which might be energy-dependent.^{13,14} Dispersive optical model potential was used to estimate the energy dependence of volume integrals of the isoscalar real(imaginary) and isovector real(imaginary) potential terms.¹⁴ We will assume roughly linear decrease of α and β values from 16 and 8 at $E_p = 40$ MeV up to 10 and 6 at $E_p = 200$ MeV, respectively. Due to the decrease of $W_D^{n(p)}$ with $E_{n(p)}$, possible dependence of the isovector terms on the $E_{n(p)}$ seems to be crucial.¹⁴

2. Collective Enhancement

The total nuclear level density is represented as the factorized contribution of quasiparticle and collective states,¹⁵ quasiparticle level densities $\rho_{qp}(U, J, \pi)$ were calculated with a phenomenological model by Ignatyuk et al.,¹⁶ which takes into account shell, pairing and collective effects, i.e.

$$\rho(U, J, \pi) = K_{rot}(U, J)K_{vib}(U)\rho_{qp}(U, J, \pi), \quad (1)$$

where $K_{rot}(U, J)$ and $K_{vib}(U)$ are factors of rotational and vibrational enhancement. At saddles and ground state deformations $K_{rot}(U, J)$ is defined by the deformation order of symmetry, adopted from Shell Correction Model calculations by Howard & Möller.¹⁷ For deformed axially symmetric nuclei (actinide nuclei at equilibrium deformations, at outer saddle deformations and neutron-deficient nuclei ($N \leq 144$) at inner saddle deformations) we assume

$$K_{rot}^{ax}(U) = \sigma_{\perp}^2 = F_{\perp} t, \quad (2)$$

where σ_{\perp}^2 is the spin cutoff parameter, F_{\perp} is the nuclear momentum of inertia (perpendicular to the symmetry axis), which equals the rigid-body value at high excitation energies, t is thermodynamic temperature. For triaxially asymmetric nuclides (inner saddle deformations) one gets

$$K_{rot}^{tax}(U) = 2\sqrt{2\pi}\sigma_{\perp}^2\sigma. \quad (3)$$

Here, $\sigma^2 = F_{\parallel} t$ is the spin distribution parameter, $F_{\parallel} = 6/\pi^2 < m^2 > (1 - 2/3\varepsilon)$, where $< m^2 >$ is the average value of the squared projection of the angular momentum of the single-particle states, ε is quadrupole deformation parameter.

Adiabatic approximation, when Eq. (1) holds, is valid up to critical energy U_r . At higher energies damping of rotational modes was anticipated by Hansen and Jensen.¹⁸ The damping of rotational modes with excitation energy might be different for axially symmetric and triaxial nuclei, then:

$$\begin{aligned} K_{rot}^{ax}(U) &= (\sigma_{\perp}^2 - 1)F(U) + 1, \\ K_{rot}^{tax}(U) &= K_{rot}^{ax}(U)((2\sqrt{2\pi}\sigma - 1)F(U) + 1). \quad (4) \\ F(U) &= (1 + \exp(U - U_r)/d_r)^{-1}. \quad (5) \end{aligned}$$

We would check Hansen and Jensen¹⁸ assumption that U_r and d_r are dependent on deformation as $\sim \varepsilon^2$, since for actinides there would be no damping of collective modes for fission saddle deformations up to $U \sim 200$ MeV.

The shell effects in level density are modelled with the shell correction dependence of a -parameter as recommended by Ignatyuk et al.¹⁶ We assume that \tilde{a} -values for equilibrium \tilde{a}_n and fission saddle \tilde{a}_f deformations are equal. That means, that a_f/a_n ratio of fissioning and residual nuclei is solely dependent upon respective shell correction values of δW ¹⁹.

III. Analysis

1. Neutron-induced Fission

Calculated fission cross section of $^{238}\text{U}(n, f)$ is compared with data on Fig 1. Assuming there is no damping at saddle deformations, $^{238}\text{U}(n, nf)$ reaction makes major contribution to σ_{nf} , which is largely overestimated for $E_n \geq 30$ MeV. When damping is assumed, major contribution comes from first ~ 10 fissioning nuclei, but measured data again are overestimated. We assume rather strong damping both at equilibrium and saddle deformation, i.e. $U_r = 20$ MeV and $d_r = 5$ MeV. Damping of collective modes leads only to reduction of contribution of predecessors (lower chance fission) and to the increase of that of successors (higher chance fission). Another major parameter of which fission cross section depends above excitations of ~ 20 MeV is the a_f level density parameter at saddle deformations. Decreasing it by $\sim 10\%$ we could describe the $^{238}\text{U}(n, f)$ data trend. In that case we could reduce the contribution of predecessors as well as successors, so the net effect is decreased calculated σ_{nf} . In case of nuclide of still lower fissility, ^{232}Th , the peculiarities observed for $^{238}\text{U}(n, f)$ reaction are even more pronounced (see Fig. 2). The description of $^{235}\text{U}(n, f)$ cross section is shown on Fig. 3. In that case dumping of collective modes allows to describe σ_{nf} of $^{235}\text{U}(n, f)$, which is ~ 100 mb higher than that of $^{238}\text{U}(n, f)$ for $E_n \geq 100$ MeV. Decreasing a_f parameter at saddle deformations by $\sim 10\%$ decreases σ_f to the level observed for the $^{238}\text{U}(n, f)$ reaction.

Fission cross section data²⁾ trends for higher fissility target $^{240}\text{Pu}(n, f)$ (see Fig. 4) and for the other lower fissility targets $^{242}\text{Pu}(n, f)$ and $^{244}\text{Pu}(n, f)$ (see Fig. 5) could be reproduced up to $E_n \sim 200$ MeV. The dependence of observed fission cross section on the fissility of the target nuclide is reproduced in the same manner as for the ^{235}U and ^{238}U targets. Total fission cross section is almost insensitive to damping of collective rotational modes at $E_n \gtrsim 70$ MeV. Relative contributions of (n,xf) reactions are rather dependent on damping strength both at saddle and equilibrium deformations, as well as survival probability against fission.²⁰⁾

2. Proton-induced Fission

Neutron- and proton-induced fission cross sections of actinide target nucleus ^{238}U are compared up to $E_{n(p)} \sim 200$ MeV on Fig. 6. Data on $^{238}\text{U}(p, f)$ reaction are much more ambiguous than those for the $^{238}\text{U}(n, f)$ reaction.⁴⁾ It might be assumed that $^{238}\text{U}(p, f)$ reaction is not much different from $^{238}\text{Np}(n, f)$ at $E_{n(p)} \geq 40$ MeV. However, above emissive fission threshold relative contributions of non-emissive fission to total fission cross section are important. Description of charge exchange reaction $^{238}\text{U}(p, n)$ and $^{238}\text{U}(p, 3n)^{236}\text{Np}$ cross sections might be considered as a validation of the consistency

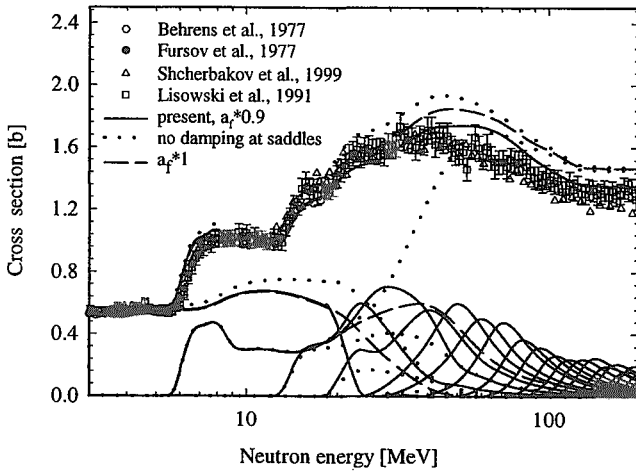


Fig. 1 ²³⁸U fission cross section

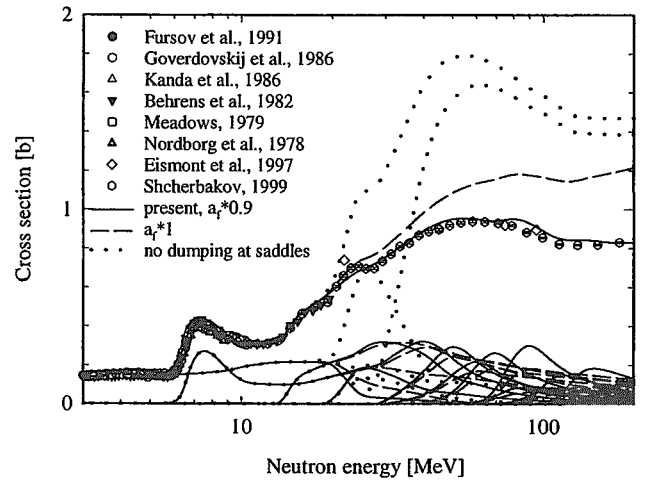


Fig. 2 ²³²Th fission cross section

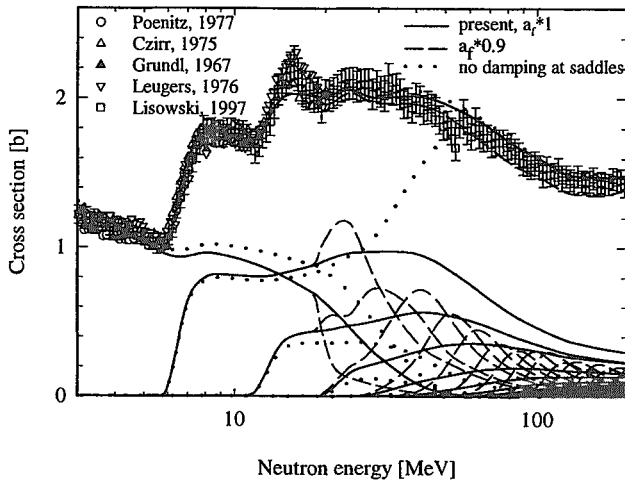


Fig. 3 ²³⁵U fission cross section

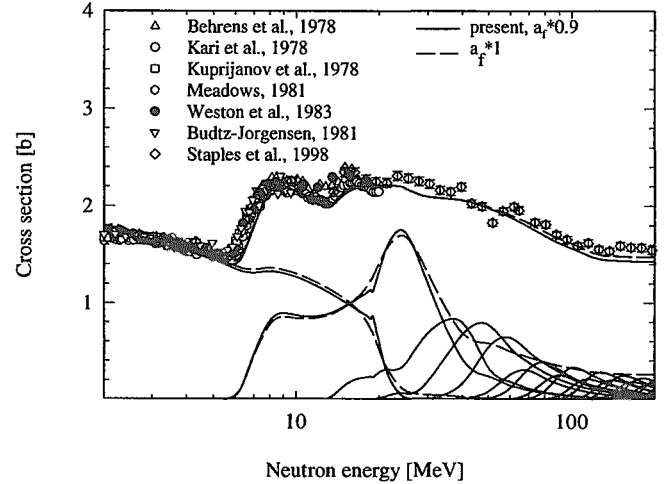


Fig. 4 ²⁴⁰Pu fission cross section

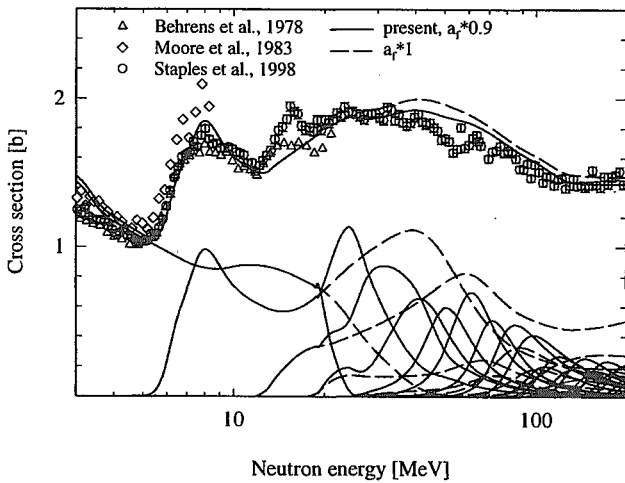


Fig. 5 ²⁴⁴Pu fission cross section

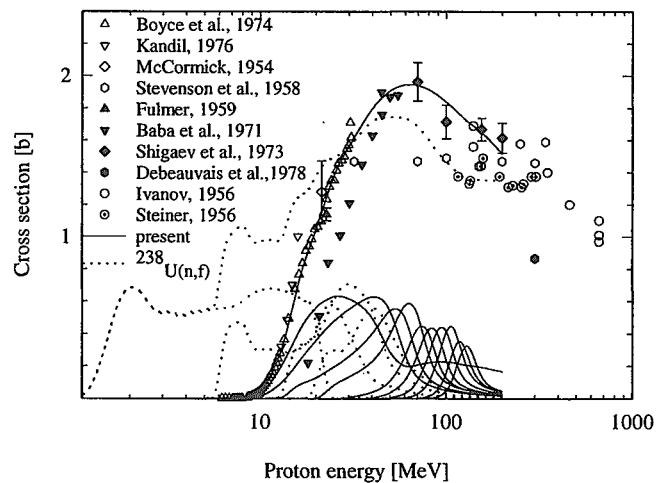


Fig. 6 ²³⁸U (p,f) cross section

of the statistical estimate of first chance fission cross section.²¹⁾ We can compare the contributions of first chance fission to the fission cross section of compound nuclide ^{239}Np for $^{238}\text{U}(p,f)$ and $^{238}\text{Np}(n,f)$ reactions. Fission of ^{239}Np nuclei might be complemented with the analysis of $^{237}\text{Np}(n,f)$ reaction cross section data,³⁾ fission probability of ^{239}Np is defined elsewhere.²²⁾ Analysis of relative contributions of first chance fission to the total fission cross section for $^{238}\text{Np}(n,f)$, $^{238}\text{U}(n,f)$ and $^{238}\text{U}(p,f)$ reactions shows that in case of p -induced fission contribution of non-emissive fission to total fission cross section is much higher than in case of n -induced fission. Specifically, above (n,2nf) reaction threshold difference amounts to $\sim 50\%$. Calculated $^{238}\text{U}(p,f)$ cross section describes reliable measured data up to $E_p \sim 40$ MeV, at higher E_p there is a large scatter of the data points.⁴⁾ The older measured data predict the lower (p,f) cross section level, roughly the same as that of (n,f) cross section. To describe the lower level (p,f) cross section one needs lower absorption cross section. For that one needs very low isovector terms of the real volume V_R^p and surface imaginary W_D^p potential. Adopted estimates of α and β parameters give an estimate of $^{238}\text{U}(p,f)$ cross section which is systematically higher than that of $^{238}\text{U}(n,f)$ reaction above projectile energy of ~ 30 MeV.

IV. Conclusions

In summary, statistical theory approach seems to be adequate for the description of neutron-induced fission cross sections of U, Np and Pu target nuclides up to $E_n \sim 200$ MeV. Calculated fission cross section approaches asymptotically absorption cross section. We have observed that with increasing fissility of target nucleus the smearing of step-like structure occurs at lower incident neutron energies E_n . Actually, this energy is the lower, the higher is the fissility of target nucleus. We argue the validity of fission/evaporation mechanism for nucleon-induced fission of actinide target nuclides up to ~ 200 MeV excitation energy. Collective modes damping independent on the deformation produces reasonable partitioning of observed fission cross section into emissive fission chances. Further decrease of fission intrinsic level densities decreases the contributions of lower chances and increases the contribution of higher chances, but to a lesser extent. The net effect is the decrease of observed fission cross section. Reliable data for the other U and Pu targets would allow to check the influence of fission barriers of neutron-deficient nuclides in the vicinity of neutron shell $N=126$ on σ_{nf} . The influence of changing shape of nuclei in the vicinity $N=126$ shell from a deformed to spherical also might be important. We anticipate that semi-empirical finding - lowering of α_f at $U \gtrsim 20$ MeV might be perceived as a lumped effect of these factors. The dependence of observed fission cross section on the projectile at $E_{n(p)} \geq 40$ MeV is interpreted as being due to optical reaction cross section difference. We observe the dependence of the first chance fission contribution to the measured fission

cross section on the projectile. It is much higher for (p,f) than for (n,f) reaction. We argue that this effect is essentially due to the dependence of the secondary neutron spectra on the projectile, rather than influence of the fissilities of fissioning nuclei.

Acknowledgment

This work was supported by the International Science and Technology Center under the Project B-404 "Actinide Nuclear Data Evaluation", Funding Party Japan.

References

- 1) P. Lisowski, A.D. Carlson, O.A. Wasson et al., *Proc. Specialists' Meeting on Neutron Cross Section Standards for the Energy Region above 20 MeV*, Uppsala, Sweden, 21-23 May, 1991, p. 177, OECD, Paris (1991).
- 2) P. Staples, K. Morley, *Nucl. Sci. Eng.* **129**, 149 (1998).
- 3) O.A. Shcherbakov et al., *Proc. of 8th Int. Seminar on Neutron Interactions with Nuclei*, Dubna, Russia, 17-20 May, 2000, p.268 (2000).
- 4) V.P. Eismont, A.I. Obukhov, A.V. Prokofyev and A.N. Smirnov, *Proc. of the Second Int. Conf. on ADTT*, Kalmar, Sweden, June 3-7, 1996, p.592 (1997).
- 5) H. Conde, V.P. Eismont, K. Elmgren, A.I. Obukhov, A.N. Smirnov, In: [4], p.599.
- 6) V.M. Maslov, IAEA-TECDOC-1034, p.81, 1998, Vienna.
- 7) V.M. Maslov, INDC(BLR)-013, IAEA, Vienna, 1998.
- 8) M. Uhl, B. Strohmaier, IRK-76/01, IRK, Vienna (1976).
- 9) V.M. Maslov and Yu.V. Porodzinskij, JAERI-Research, 98-038, 1998.
- 10) R.L. Shutt, R.E. Shamu, P.W. Lisowski et al., *Phys. Lett.* **B203**, 22 (1988).
- 11) P.G. Young, IAEA-TECDOC-1034, p.131, 1988, Vienna.
- 12) V.M. Maslov, Yu.V. Porodzinskij, A. Hasegawa and K. Shibata, JAERI-Research, 98-040, 1998.
- 13) D. Madland, *Proc. of the Spec. Meeting on Nucleon-Nucleus Optical Model up to 200 MeV*, 13-15 Nov., 1996, Bruyeres-le-Chatel, France, p. 129 (1997).
- 14) J.P. Delaroche, E. Bauge, P. Roman, *Proc. Int. Conf. Nucl. Data for Sci. and Techn.*, Trieste, Italy, May 19-24, 1997, p. 206 (1997).
- 15) A. Bohr and B. Mottelson, *Nuclear Structure*, vol. 2, (Benjamin, New-York, 1975).
- 16) A.V. Ignatjuk, K.K. Istekov, G.N. Smirenkin, *Sov. J. Nucl. Phys.*, **29**, 450 (1979), [in Russian].
- 17) W.M. Howard, P. Möller, *Atomic Data and Nuclear Data Tables*, **25**, 219 (1980).
- 18) G. Hansen, A.S. Jensen, *Nucl. Phys.* **A406**, 236, (1983).
- 19) W.O. Myers, W.J. Swiatecky, *Ark. Fyzik*, **36**, 243 (1967).
- 20) A.R. Junghans et al., *Nucl. Phys.*, **A629**, 635 (1998).
- 21) V.M. Maslov, *Sov. J. Atomic Energy*, **69**, 878 (1990).
- 22) V.M. Maslov, Yu.V. Porodzinskij et al., INDC(BLR)-011, IAEA, Vienna, 1998.